PFG 2011 / 4, 0233 – 0245
Stuttgart, August 2011

Article

Object-based Change Detection

Clemens Listner & Irmgard Niemeyer, Jülich

Keywords: Change Detection, Multivariate Alteration Detection, Multiresolution Segmentation, Object-based Image Analysis, Neural Networks

Summary: The iteratively reweighted multivariate alteration detection (IR-MAD) has shown to be a very useful tool for detecting changes in imagery acquired over the same area but at different times. However, applying the paradigm of object-based image analysis (OBIA) leads to the problem how to connect corresponding objects extracted from images recorded at two different times. Moreover, the huge number of object features available in OBIA results in numerical instabilities within the MAD method due to near-singular covariance matrices. The paper introduces recent developments for object-based change detection. First, a new approach to segmentation for object-based change detection will be presented: The algorithm segments the first image using the multiresolution segmentation. Assigned to the second image, all segmentation merges are checked for consistency and removed if the check fails. Second, the paper shows how to address the numerical problems in the MAD algorithm by regularisation as well as by dimensionality reduction using Principal Component Analysis (PCA). It will be demonstrated how to integrate the adapted segmentation andIR-MAD into the object-based change detection workflow.

Zusammenfassung: *Objekt-basierte Änderungsdetektion*. Die Methode der Iteratively Reweighted Multivariate Alteration Detection (IR-MAD) hat sich als sehr nützliches Instrument erwiesen, um Änderungen zwischen zwei Satellitenbildern unterschiedlicher Aufnahmezeiten eines Gebietes zu analysieren. Jedoch kann die Methode nicht direkt den Ansatz der objektbasierten Bildanalyse (OBIA) integrieren. Insbesondere ist es bisher nicht möglich Änderungen der Form zwischen den Bildern zu detektieren, da die Algorithmen zur Objektextraktion, der so genannten Segmentierung, nicht robust genug sind. Darüber hinaus führt die durch das OBIA-Konzept verfügbare große Anzahl untereinander korrelierter Objekteigenschaften dazu, dass die Methode der IR-MAD numerisch instabil wird. Diese Arbeit präsentiert zwei Neuentwicklungen im Bereich der objekt-basierten Änderungsdetektion. Einerseits wird ein Algorithmus zur Bildsegmentierung vorgestellt, der es ermöglicht, die IR-MAD-Methode direkt auf Basis der Objekte durchzuführen. Andererseits zeigt diese Arbeit auf, wie die numerischen Probleme der IR-MAD-Methode durch Regularisierung und Dimensionsreduktion mittels Hauptkomponentenanalyse gelöst werden können.

1 Introduction

Change detection has always been an important application for remote sensing data. It may be defined as the analysis of two or more images of the same area but acquired at different times in order to identify significant changes of or at the earth's surface. Change detection techniques are being used in a variety of fields, such as disaster management, forestry monitoring, water level monitoring, infrastructure planning, and many more.

According to the broad range of change detection applications using remote sensing data, also a huge number of data processing methods were proposed (Singh 1989, Lu et al. 2004, Radke at al. 2005, Canty 2009): Methods analysing difference images, classification-based approaches and kernel-based methods such as principal component analysis or multivariate alteration detection, to name just a few examples. All these approaches have in common that they compare corresponding image pixels of different acquisition times.

www.schweizerbart.de
DOI: 10.1127/1432-8364/2011/0085
1432-8364/11/0085 $ 3.25

However, due to the increased spatial resolution of remote imaging sensors, the aggregation of similar neighbouring pixels into homogeneous objects has become more and more popular. After the aggregation, also referred to as segmentation, the user might consider also shape, relations and texture of the image objects in the analysis. This paradigm is called object-based image analysis (OBIA) (Blaschke et al. 2008). Change detection can also be carried out based on the image objects. A number of studies showed the application of object-based approaches for detecting surface changes between different acquisition times.

1.1 *Segmentation Adapted for Object-based Change Detection*

Earlier studies (Niemeyer et al. 2008, 2009) turned out that segmentation is the crucial step in object-based change detection. For image data taken over the same area at two different acquisition times, the image segmentation could be generally performed in three different ways:

a) On the basis of the bi-temporal data set, i. e., using a data stack consisting of both scenes;
b) based on the image data of one acquisition time; the generated object boundaries are then simply assigned to the image data of the second acquisition;
c) separately for the two times, i. e., the two data sets are segmented independently.

When using a segmentation as suggested in (a) or (b), the resulting image objects have the same geometric properties at the two times, i. e., time-invariant shape features. Change detection can only be applied to a limited number of time-variant object features, such as layer values, texture etc. Provided independent segmentation of the two scenes (c), also the image object geometry varies in time. In this case, all available object features could be used for object-based change detection. However, the issue of linking objects has not been solved satisfactorily yet. In summary, each of the three approaches has severe drawbacks concerning the use of shape features, segmentation robustness and quality, or the problem of linking corresponding objects of different acquisition times, see Niemeyer et al. (2008) for a more detailed discussion.

Therefore, we will present a new segmentation approach for object-based change detection. The method is based on the idea of multiresolution segmentation (Baatz & Schäpe 2000), which is a core component of the eCognition software (Definiens 2009). Given a bi-temporal dataset acquired over the same area, the adapted procedure aims to provide almost identical segments for image regions where no temporal changes occurred and different segments for temporally changed image regions.

1.2 *Object-based Techniques for Change Detection*

Some authors presented object-based classifications for change detection studies, among them for instance Zhou et al. (2008), who investigated the post-classification comparison based on traditional pixel-based versus object-based classifiers. The change map produced by the object-based method achieved a higher Kappa index of agreement (KIA) than the pixel-based method. Hese et al. (2006) reported that object-based change detection approaches taking the object shape into account could increase the classification accuracy of change classes. Conchedda et al. (2008) applied object-based post-classification comparison versus object-based change detection analysis of mangrove ecosystems and received a higher overall accuracy for the object-based post-classification comparison. Im et al. (2008) compared three different object-based change classification techniques using object/neighbourhood correlation with two different pixel-based approaches, and figured out that object based change classifications achieve higher KIA values than the pixel-based methods. Niemeyer & Nussbaum (2006) used a combination of pixel- and object-based approaches by firstly pinpointing the significant change pixels by statistical change detection, object extraction and subsequent post-classification of changes based on a semantic model of object features.

Other authors proposed change detection combining object-based classification and

geo-information systems (GIS). Walter (2004) presented a two steps approach starting with object-based classification of remote sensing data using training areas derived automatically from a GIS database. For change detection, the classified data was then compared with the existing GIS objects. Hofmann et al. (2008) implemented different change indicators based on a comparison of the input bi-temporal satellite data and used them in combination with a transition-probability-matrix to detect and reclassify potential changes of GIS-objects. Changhui et al. (2010) performed an object-based classification using support vector machines (SVM) and compared the objects with land use vector data.

Some other authors developed object-based change detection techniques employing the differences of spectral and textural object features existing at the considered acquisition times. Desclée et al. (2006) proposed a new change detection procedure, in which anomalous values of reflectance differences statistics were identified based on a chi-square test of hypothesis, and the corresponding objects were labelled as change. Lefebvre et al. (2008) presented a geometric change detection procedure based on the analysis of object contours and content change by wavelet-based texture analysis. Huo et al. (2010) combined the differences of spectral and textural object features for urban change analysis using very high-resolution optical imagery. Huang et al. (2010) compared pixel-based versus object-based change detection by integrating intensity and texture differences and found object-based change detection to be more appropriate.

Besides object class membership, spectral and textural differences, also the temporal modification of other object features could be utilised for statistical change detection. Additional layer features, like ratio, standard deviation and others, as well as relational and shape features could help to address thematic, geometric and topologic object changes between two acquisition times. Niemeyer et al. (2008, 2009) applied the regularized iteratively reweighted multivariate alteration detection (IR-MAD – Nielsen 2007) for analysing changes of image objects based on their features. The MAD transformation (Nielsen et al. 1998) was originally developed for pixel-based change detection. It is based on a classical statistical transformation of the multispectral feature space referred to as canonical correlation analysis to enhance the change information in the difference images. When applying the IR-MAD transformation to a feature space with only small correlations between the dimensions, normally no numerical issues occur. However, in datasets with high correlation between the dimensions, as it can be found in hyperspectral data or object-based processing using many features, the algorithm results in near-singular covariance matrices which cannot be inverted in a straightforward way. In this context, Nielsen (2007) proposed to reduce the dataset dimensionality and hence to decrease the correlation between the dimensions. We therefore implemented a principal component analysis (PCA) transformation into the object-based change detection process for reducing the feature space dimensions before applying the IR-MAD method.

Section 2.1 describes the multiresolution segmentation method in detail and introduces its enhancement as to object-based change detection. Section 2.2 presents the idea of the IR-MAD and shows which modifications are necessary to obtain a stable behaviour of the algorithm. Section 2.3 briefly reviews the use of class-based feed-forward networks and Section 2.4 shows the change detection workflow. Investigations on the suggested segmentation procedure are presented in Section 3.1, followed by the discussion of three change detection experiments using different approaches in Section 3.2. Section 4 gives some general conclusions.

2 Methods

2.1 *Multiresolution Segmentation Adapted for Object-based Change Detection*

The general idea of our work is to create segmentations of the two images I_1 and I_2, acquired at different times over the same area, that only differ in image regions where actual changes took place. For this purpose we adapted a region-growing segmentation algorithm

called multiresolution segmentation (Baatz & Schäpe 2000), which is available in the eCognition software for object-based image analysis (Definiens 2009). The multiresolution segmentation starts with pixels as initial segments and iteratively aggregates neighbouring segments to bigger segments according to predefined heterogeneity criteria.

However, object-based change detection requires a segmentation technique that similarly extracts objects that have not changed their shape and size between the two acquisition times. The multiresolution segmentation implemented in the eCognition software uses homogeneity criteria based on color and shape, and a scale parameter in combination with local and global optimization techniques. Thus, applying the same segmentation parameters to both scenes does hardly produce similar objects in image regions with no or negligible changes, if other parts of the image have slightly changed.

In our procedure, the multiresolution segmentation is used to generate a segmentation of I_1. After that, the segmentation is also applied to I_2 and tested for its consistency. If a segment is found to be inconsistent with I_2, it will be split up. But let us start with describing the multiresolution segmentation in more detail, before introducing the adaption for change detection.

Multiresolution segmentation is a region-based approach. In this approach, segments can be considered as binary trees in which the leaf nodes correspond to single pixels and every merge step can be represented by a non-leaf node. According to this model, we will use the terms segment and node synonymously throughout this paper.

The multiresolution segmentation starts with an initial chessboard segmentation that identifies each pixel as an individual segment. Then, segments grow in multiple cycles. In each cycle a random seed S_1 of minimal tree depth is selected iteratively in order to check if one of its neighbours S_2 can be merged with S_1 to a new segment S_{new}. The degree of fitting is modelled by the measure of heterogeneity h that has to fulfil

$$h(S_{new}) < T, \tag{1}$$

T being a given threshold. The aim is to minimize h in the neighbourhood of S_1 when being merged with S_2. Furthermore, S_1 has also to minimize h in the neighbourhood of S_2. Otherwise, S_2 is set to be the next seed. This strategy, called *local mutual best fitting* (see Fig. 1), results in a path of descending values for h leading to a local minimum. Hence, it is impossible to run into an infinite loop. Moreover, this strategy causes a regular growth of the segments. For specific formulas on the heterogeneity measure, see (Listner & Niemeyer 2010).

If no local mutual best fitting neighbour has been found given seed S_1, it is marked as final. Final segments can no longer be merged with other segments until the end of a segmentation cycle or a merge of neighbouring segments. If all segments have been marked as final, the algorithm continues with the next cycle by resetting all segments from final. The algorithm ends if none of the present segments has been merged with another segment during a cycle.

In case a single image is being segmented, the information about the child segments has no further relevance after merging them.

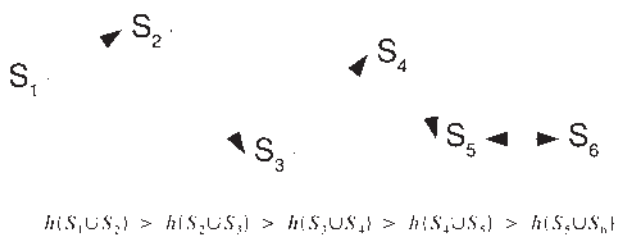

Fig. 1: Local mutual best fitting strategy.

However, as we intend to test the segmentation of one acquisition time for consistency with an image of another acquisition time, the information on the segment history, i. e., the segment hierarchy, needs to be saved within the process. Depending on the applied consistency tests, also information on the neighbourhood existing at the time a segment was created could be necessary (Listner & Niemeyer 2010).

Following the insight into the multiresolution segmentation algorithm, we now focus on adapting this algorithm to the problem of segmenting two images of the same area acquired at different times. We therefore propose the following approach:

1. Segment image I_1 using the multiresolution segmentation algorithm.
2. Apply this segmentation to image I_2 and recalculate the heterogeneity of each segment based on the data of I_2.
3. Check every merge, i. e., every segment that consists of more than one pixel, for consistency by applying a test criterion. Not only the top-level segments, i. e., the nodes without parents, need to be examined but all nodes in each segment tree except for the leaf nodes.
4. Remove all inconsistent nodes using a segment removal strategy.
5. Re-run the multiresolution segmentation to obtain a final segmentation of the second image.

These steps present a general process which has to be specified in two aspects. First, how can segments of image I_1 be checked for consistency with image I_2 and second, how can inconsistent segments be removed?

With regard to the consistency tests we propose three different criteria. The first one, named *threshold test*, examines whether a given segment S fulfils the condition

$$h(S) < T_{check}. \tag{2}$$

Otherwise the segment S is marked as inconsistent. The threshold test is the weakest test with respect to changes between the two images.

The second test, called *local best fitting test*, tries to repeat the merge procedure with the data of image I_2. Given an exemplary segment structure with parent segment S_3 and its children S_1 and S_2, the test assumes S_1 to be a seed and searches for locally best fitting neighbours from the list of merge candidates that has been stored during the segmentation of image I_1. If the best fitting neighbour is S_2, the test is passed, otherwise it is failed. Besides, also the condition given in Equation 2 needs to be fulfilled. Obviously, this test is very sensitive even to small changes or noise in the imagery. In order to reduce the sensitivity of the test, a parameter $T_{checktolerance}$ is introduced. The idea of this additional parameter is that a merge may not be the locally best fitting one but could belong e. g., to the 10% best fitting ones. Therefore the test checks how many merge candidates perform better (n_{better}), equally well (n_{equal}) and worse (n_{worse}) than the segment that has been merged to the seed. If the condition

$$\frac{n_{better}}{n_{better} + n_{equal} + n_{worse}} < T_{checktolerance} \tag{3}$$

holds, the consistency test is considered to be passed.

Finally, the third test is named *local mutual best fitting test*. It also tests if S_2 is the best fitting neighbour for seed S_1 in the list of merge candidates but checks additionally if S_1 is the best fitting neighbour for S_2. This test's principle is derived from the idea of local mutual best fitting presented before. Compared to the local best fitting test, this test is more sensitive; however, applying Equation 3 could also reduce the sensitivity of this test. In general, splitting-up segments could be avoided by increasing threshold T_{check}. Then, not all changes between I_1 and I_2 may result in changes of the segmentation.

After testing all given segments for consistency with the image I_2, those segments that did not pass the test have to be handled. We therefore introduce three strategies to remove these segments.

The first strategy is named *universal segment removal strategy*. The principal idea of this strategy is illustrated in Fig. 2: It searches for the top-level segment of an inconsistent segment and splits it into its elements. As a result, only pixel segments will remain. Obviously, this strategy affects the segmentation intensively and could therefore create changes

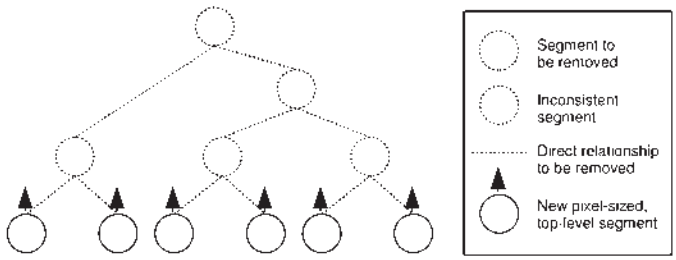

Fig. 2: Universal segment removal strategy.

in the final segmentation in areas where no actual changes can be observed.

The second strategy for removing inconsistent segments is the *global segment removal strategy*. Its basic principle, as illustrated in Fig. 3, is to remove the inconsistent segment and all its ancestors from the segment tree. During this process all remaining segments are considered to be new top-level segments. In this way, the impact on the segment tree is reduced. However, this strategy is very adaptive in creating changes only in parts of the segment tree in which changes can be detected and leaves the rest as it is.

The third and most complex segment removal algorithm is called *local segment removal strategy*. It is developed due to the fact that the global segment removal strategy affects parts of the segment tree which do not necessarily change between different acquisition times. Consider for example a big object in image *I1* which is segmented correctly. If only a small part of this object changes from one acquisition time to another, it may be a better to extract this small part instead of splitting up the whole object.

Therefore we propose an additional method for removing inconsistent segments: Assume *I*

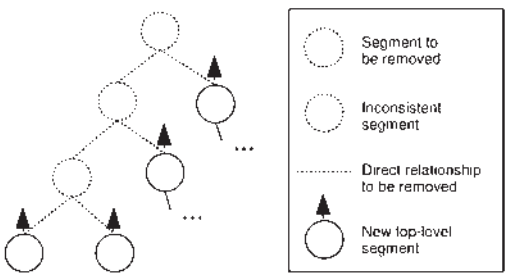

Fig. 3: Global segment removal strategy.

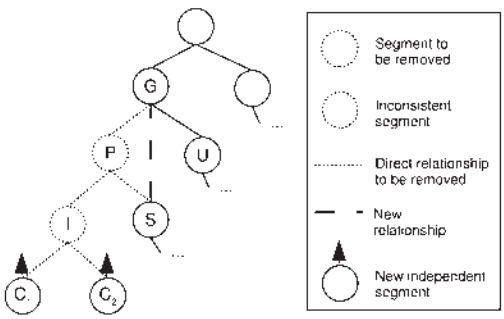

Fig. 4: Local segment removal strategy.

to be an inconsistent node. Then remove *I* and its parent *P* from the segment tree. Set *I's* children C_1 and C_2 as top-level segments and put *I's* sibling *S* as child of *I's* grandparent *G*. This method is illustrated in Fig. 4. It has turned out that the local segment removal strategy cannot be applied directly in all possible constellations. See Listner & Niemeyer (2010) for a detailed discussion of this issue.

In this section we have shown some ideas for addressing the problem of segmentation for object-based change detection. These ideas were implemented using the C++ programming language including STL (see Musser 1995) and GDAL (see GDAL 2010).

2.2 *IR-MAD Adapted for Object-Based Change Detection*

The IR-MAD method is a linear transformation of the feature space aimed at enhancing the change information in the difference image. It models an object's feature vector as random vectors *F* and *G* of length *N* with *F* representing the information from the first and *G* from the second image. It then uses the corresponding covariance matrices Σ_{FF}, Σ_{FG} and Σ_{GG} to calculate the transformation vectors *a* and *b* as the solution of the generalized coupled eigenvalue problem

$$\begin{aligned}\Sigma_{FG}\Sigma_{GG}^{-1}\Sigma_{FG}^{T}a &= \rho^2\Sigma_{FF}a,\\ \Sigma_{FG}\Sigma_{FF}^{-1}\Sigma_{FG}^{T}b &= \rho^2\Sigma_{GG}b.\end{aligned} \tag{4}$$

Solving this problem yields *N* solutions with eigenvectors a_i and b_i and corresponding eigenvalues ρ_i sorted in ascending order. Using this result, the transformed difference images M_i is calculated as

$$M_i = U_i - V_i = a_i^T F - b_i^T G. \tag{5}$$

It can be shown that M_1 has maximum variance and thus U_1 and V_1 minimum correlation under the constraint that *Var(U)=Var(V)*=1. The transformed imagery emphasizes the differences between the two acquisition times. Moreover, the M_i's, referred to as MAD components, are mutually uncorrelated which has the effect that different components show different types of changes. The sum of squares of standardized variates is approximately chi-square distributed with *N* degrees of freedom. Supposing that no-change pixels have a chi-square distribution with *N* degrees of freedom, *N* being the number of MAD components, the change-probability can be derived for each pixel or object. For a more comprehensive explanation of the IR-MAD method see (Nielsen 2007, Canty 2009).

As the covariance matrices have to be estimated from the imagery, they may not always be invertible (Nielsen 2007). However, Equation 4 requires the inversion of Σ_{FF} and Σ_{GG}. Therefore, we propose to reduce the dimensionality of the data using the principal component analysis (PCA). Principal component analysis is a linear transformation like the IR-MAD method. The difference to IR-MAD is that PCA operates on a single dataset which is modelled by a random vector *F*. Based on this vector's covariance matrix ΣF, the eigenvalue problem

$$\Sigma_F a = \rho a. \tag{6}$$

is solved. This yields *N* pairs of eigenvalues *ai* and corresponding eigenvectors ρ_i sorted in descending order, that are then used to carry out the transformation

$$U_i = a_i^T F. \tag{7}$$

It can be shown that the variance is maximized for U_i under the constraint that $|a_i|$=1 and that U_i is not correlated to any component U_j with $j<i$. The variance of the single components is given by

$$Var(U_i) = \rho_i . \tag{8}$$

For more information on PCA see (Canty 2009). Hence, only those components containing a significant high variance are used for further analysis, the remaining features are ignored.

In practice, we estimate the covariance matrix Σ_F by using both images. Then the imagery is transformed and the features $U_1,...,U_M$ are selected if they describe at least 95% of the total variance, i. e.,

$$\sum_{i=1}^{M} Var(U_i) \Big/ \sum_{i=1}^{N} Var(U_i) \geq 0.95. \quad (9)$$

Both IR-MAD and PCA transformation were programmed using the Newmat C ++ matrix library and Numerical Recipes Software and implemented as eCognition Developer plug-in using the eCognition Software Development Kit (SDK).

2.3 *Classification of Object Changes Using Neural Networks*

In earlier studies (Marpu 2009, Niemeyer et al. 2009), two different two-layered feed forward network topologies were tested for object-based classification: Standard feed forward network (FFN) and the so-called class-based feed forward network (CBFFN). The new architecture of CBFFN was developed using the feed forward neural networks to especially facilitate the handling of the huge feature space within the object-based image analysis and to automatically extract the relevant object features. This architecture is named class-based as the output of the individual class-related FFNs defined in the architecture only use the characteristic features of the particular classes and make a final decision in the end. The proposed architecture consists of two layers of neural networks. In the first layer there are exactly K networks NN_k representing K classes. The network representing class k is only fed with the characteristic features of that class. The output of each network represents a fuzzy value of each class which are then fed as input to the second layer network. The second layer network finally gives a class membership probability for every class. Three learning algorithms and two combinations for a two-layered feed forward network (FFN) were used: Backpropagation, Kalman filter training, scaled gradient conjugated (SCG), Kalman filter and backpropagation, Kalman filter and SCG. The two network topologies with the five learning algorithms were programmed and implemented as eCognition Developer plug-in using the eCognition Software Development Kit (SDK) and IT++ library. For more detailed information, please see (Marpu 2009, Niemeyer et al. 2009).

2.4 *Object-Based Change Detection Workflow*

Using the segmentation as described in Section 2.1, it is possible to retrieve a segmentation of the imagery with at least three advantages: Firstly, we are now able to integrate shape features into the change analysis. Secondly, the presented segmentation algorithm is robust as it only leads to a different segmentation of image I_2 in areas where using the segmentation of I_1 would not be consistent with the data of I_2. Thirdly, the segmentation results have a high quality because it is not necessary to produce a single segmentation taking both images I_1 and I_2 into account. However, we still receive separate object layers for either acquisition time, which have to be connected in order to obtain a correspondence between the image objects. Corresponding objects are required for applying the IR-MAD transformation, since the IR-MAD algorithm models the objects from I_1 and I_2 as realisation of random feature vectors F and G respectively. Hence, we need to estimate the parameters using corresponding realisations of F and G. For that reason we will propose two procedures on how to establish a one-to-one relationship between the segmentations of image I_1 and I_2.

The first procedure, named *directed object correspondence*, associates each segment S_i in I_1 with all segments $T_1,...,T_n$ in I_2 that are overlapping S_1. Since this would not establish a one-to-one relationship, we set the realisations of X and Y to

$$\begin{aligned} x_i &= f_x(S_i), \\ y_i &= \frac{1}{n}\sum_{k=1}^{n} f_y(T_k), \end{aligned} \quad (10)$$

where f_x and f_y are functions returning the feature vectors of a given segment in the image I_1 and I_2 respectively. Thus, a pair of values (x_i,y_i) is available for every segment S_i in image I_1. This result can now be used to estimate the probability distribution's parameters. An example for a specific object constellation illustrating the method is given in Fig. 5a.

The second procedure for establishing an object-to-object relationship between the segmentations of image I_1 and I_2 is called *corre-*

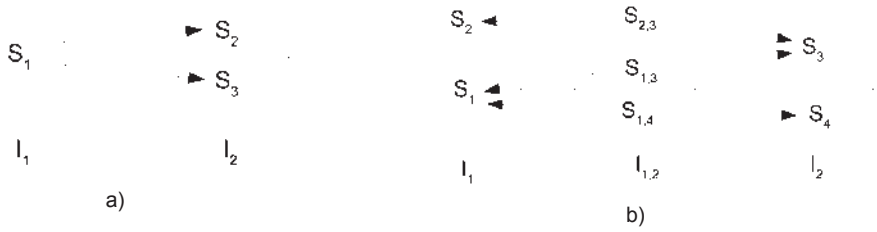

Fig. 5: Object correspondence: a) Directed, b) via intersection.

spondence via intersection. The main idea of this method is to construct a third segmentation by intersecting segments from the segmentations of I_1 and I_2. Given the segments S_1 from the segmentation of I_1 and S_2 from the segmentation of I_2, a segment $S_{1,2}$ is constructed by

$$S_{1,2} = S_1 \cap S_2. \tag{11}$$

This automatically involves a unique correspondence of $S_{1,2}$ in the images I_1 and I_2. Hence, the realisations of X and Y can be calculated straightforwardly for each segment $S_{1,2}$ by

$$\begin{aligned} x_i &= f_x(S_1), \\ y_i &= f_y(S_2). \end{aligned} \tag{12}$$

An example for the application of the method for *object correspondence via intersection* is given in Fig. 5b.

3 Experiments

Some experiments were carried out using bi-temporal RGB aerial imagery, acquired over a German motorway with a time difference of 0.7s. This particular dataset was selected to focus on the specific changes (here: vehicles movement) and to limit false alarms due to illumination and/or seasonal changes at the two acquisition times. However, some false alarms may result from sensor noise, different acquisition angles and registration inaccuracy. The two images were radiometrically normalised using the automatic techniques proposed by Canty & Nielsen (2008) and Median filtered.

3.1 *Segmentation*

The segmentation was carried out using the adapted multiresolution segmentation presented in Section 2.1. The *threshold test and the universal segment removal strategy* turned out to provide the best results for our study.

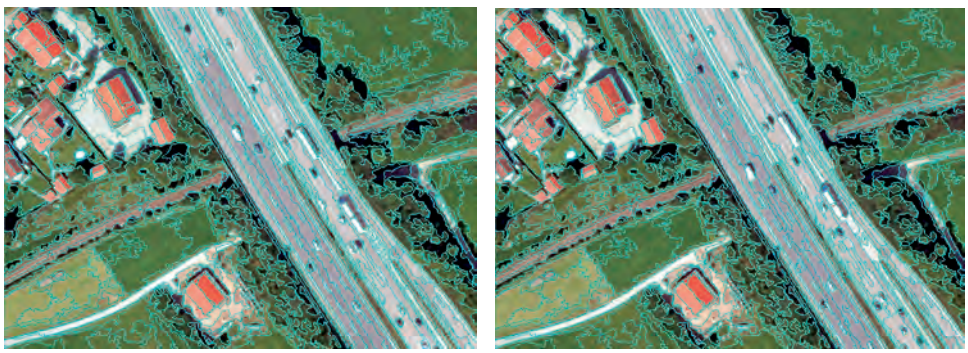

Fig. 6: Segmentation of the bi-temporal imagery using the threshold test and the universal segment removal strategy.

Fig. 6 shows the results for the two acquisition times. The procedure similarly extracted objects that have not changed their shape and size on both sides of the motorway and provided different results for the motorway.

3.2 *Change Detection*

The change detection procedure was tested using the eCognition Developer software with three different configurations. In the first experiment, hereinafter referred to as *directed change detection*, the changes were estimated in either directions, i. e., from time 1 to time 2 and from time 2 to time 1. The second experiment applied the object correspondence via intersection and will be named *change detection using intersected objects* in the following. The third experiment, entitled *change detection using MAD objects*, conducted the IR-MAD on the image pixels and continued with an object-based classification using neural networks.

For the *directed change detection*, the two results from the adapted multiresolution segmentation (Fig. 6) were used. Corresponding image objects in either time were connected applying the directed object correspondence. Ten object features were selected: Compactness as shape feature, object mean color, object standard deviation and the object mean of the grey level co-occurrence matrix (GLCM, texture feature) of the three given bands. After the PCA transformation, the first three PCs were taken as input for the IR-MAD. Finally, the object classes "no change" and "change" were classified using the class-based neural network (CBFFN) procecure applying the SCG and Kalman filter as combined learning algorithm. Fig. 7 shows the results for the changes from time 1 to time 2 (left) and vice versa (right).

The approach *change detection using intersected objects* again used the two results from the adapted multiresolution segmentation as input, but applied a different method for connecting objects, namely the object corresponce via intersection. In addition to the object features employed in the previous experiment, also the shape index was used as input for the PCA. As before, the first three PCs were used as basis for the IR-MAD. The MADs and the chi square values were then taken as input for classifying the classes "no change", "time 1" and "time 2" using CBFNN (Fig. 8).

Finally, the third experiment named *change detection using MAD objects* took yet another approach. Starting with a pixel-based IR-MAD, the three MADs were taken as input for segmenting the image objects. 15 features were selected: Mean, standard deviation and mean difference to neighbours as spectral features and GLCM homogeneity and GLCM mean as texture features, in each case for all three spectral bands. The procedure followed similar to the first two experiments: PCA, IR-MAD and CBFFN classification. Fig. 9 gives the results.

Accuracy Assessment

The accuracy assessment of the three experiments gives high overall accuracy (0.98–0.99)

Fig. 7: Directed change detection. Changes from time 1 to time 2 (left) and from time 2 to time 1 (right).

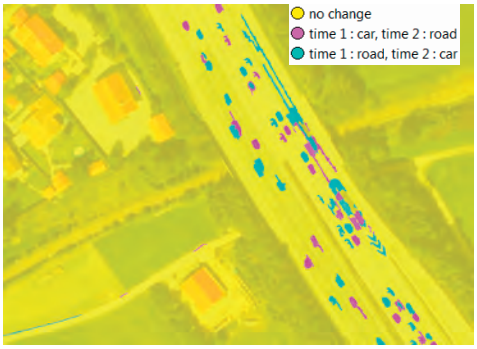

Fig. 8: Change detection using intersected objects.

Fig. 9: Change detection using MAD objects.

Tab. 1: Change detection accuracy assessment.

	Directed change detection: T1->T2		Directed change detection: T2->T1		Change detection using intersected objects		Change detection using MAD objects	
User's accuracy	No change	z0.98	No change	0.96	No change	0.99	No change	0.99
		1.00	T1: road, T2:car	0.97	T1: car, T2: road	0.78	T1: car, T2: road	0.66
					T1: road, T2:car	0.52	T1: road, T2:car	0.69
Producer's accuracy	No change	1.00	No change	0.99	No change	0.99	No change	0.99
	T1: car, T2: road	0.71	T1: road, T2:car	0.81	T1: car, T2: road	0.76	T1: car, T2: road	0.52
					T1: road, T2:car	0.94	T1: road, T2:car	0.72
Overall accuracy	0.98		0.98		0.98		0.99	
KIA	0.82		0.87		0.77		0.75	

and promising kappa coefficients (0.75–0.82) for either approach (Tab. 1). However, the user's and producer's accuracy vary for the three approaches and for the change classes.

4 Conclusion

We presented some new ideas for object-based change detection using remote sensing imagery. An enhanced procedure for segmentation was introduced and implemented into the change detection workflow. Moreover, numerically issues in the IR-MAD method were addressed. The proposed methods showed good results in three experiments using aerial imagery.

Nevertheless, further developments are needed such as new consistency tests and segment removal strategies. Moreover, methods for enabling the user to easily select the segmentation parameters, e. g., by using training samples, would be helpful. Finally, the adapted multiresolution segmentation needs to be implemented as eCognition plugin for allowing its direct use in the proposed change detection workflow.

The presented OBIA tools are available for download at www.treatymonitoring.de/tools/.

Acknowledgments

The authors would like to thank Prof. Peter Reinartz (DLR) for providing the RGB aerial imagery used for the experiments.

References

Baatz, M. & Schäpe, A., 2000: Multiresolution Segmentation: an optimization approach for high quality multi-scale image segmentation. – Angewandte Geographische Informationsverarbeitung XI. Beiträge zum AGIT-Symposium **1999:** 12–23.

Blaschke, T., Lang, S. & Hay, G. (Eds.), 2008: Object-Based Image Analysis Spatial Concepts

for Knowledge-Driven Remote Sensing Applications. Lecture Notes in Geoinformation and Cartography. – Springer, Berlin.

Canty, M.J., 2009: Image Analysis, Classification, And Change Detection in Remote Sensing: With Algorithms for ENVI/IDL. – 2nd edition, Taylor & Francis Ltd.

Canty, M.J. & Nielsen, A.A., 2008: Automatic radiometric normalization of multitemporal satellite imagery with the iteratively re-weighted MAD transformation. – Remote Sensing of Environment **112:** 1025–1036.

Changhui, Y., Shaohong, S., Jun, H. & Yaohua, Y., 2010: An Object-Based Change Detection Approach using High-Resolution Remote Sensing Image and GIS Data. – International Conference on Image Analysis and Signal Processing (IASP10): 565–569.

Concheddaa, G., Durieux, L. & Mayaux, P., 2008: An object-based method for mapping and change analysis in mangrove ecosystems. – ISPRS Journal of Photogrammetry & Remote Sensing **63:** 578–589.

Definiens Imaging, 2009: Definiens eCognition Developer 8 User Guide. Munich.

Desclée, B., Bogaert, P. & Defourny, P., 2006: Forest change detection by statistical object-based method. – Remote Sensing of Environment **102:** 1–11.

GDAL Development Team, 2010: GDAL – Geospatial Data Abstraction Library, Version 1.6.0. – Open Source. Geospatial Foundation.

Hese, S. & Schmullius, C., 2006: Object Context Classification for Advanced Forest Change Classification Strategies. – International Archives of Photogrammetry and Remote Sensing **36** (4/C42).

Hofmann, P., Lohmann, P. & Müller, S., 2008: Concepts of an object-based change detection process chain for GIS update. – International Archives of Photogrammetry and Remote Sensing **37:** 305–312.

Huang, L., Zhang, G. & Li, Y., 2010: An Object-based Change Detection Approach by Integrating Intensity and Texture Differences. – 2nd International Asia Conference on Informatics in Control, Automation and Robotics (CAR 10): 258–261.

Huo, C, Chen, K., Zhou, Z., Lu, H. & Chenga, J., 2008: Robust change detection by integrating object-specific features. – International Archives of Photogrammetry and Remote Sensing **37** (B7): 797–802.

Im, R., Jensen, J.R. & Tullis, J.A., 2008: Object-based change detection using correlation image analysis and image segmentation. – International Journal of Remote Sensing **29** (2): 399–423.

Lefebvre, A., Corpetti, T. & Hubert-Moy, L., 2008: Object-oriented approach and texture analysis for change detection in very high resolution images. – International Geoscience and Remote Sensing Symposium (IGARSS 08), (CD-Rom).

Listner, C. & Niemeyer, I., 2010: Multiresolution segmentation adapted for object-based change detection. – SPIE Europe Remote Sensing 10, Vol. 7477A, Image and Signal Processing for Remote Sensing.

Lu, D., Mausel, P., Brondizio, E. & Moran, E., 2004: Change detection techniques. – International Journal of Remote Sensing **25** (12): 2365–2407.

Marpu, P.R., 2009: Geographic Object-based Image Analysis. – PhD Thesis, Institute of Mine-Surveying and Geodesy, TU Bergakademie Freiberg.

Miller, O., Pikaz, A. & Averbuch, A., 2005: Objects based change detection in a pair of grey level images. – Pattern Recognition **38:** 1976–1992.

Musser, D.R. & Saini, A., 1995: The STL Tutorial and Reference Guide: C++ Programming with the Standard Template Library. – Addison Wesley Longman Publishing Co., Inc. Redwood City, CA, USA.

Nielsen, A.A., 2007: The regularized iteratively reweighted MAD method for change detection in multi-and hyperspectral data. – IEEE Transactions on Image Processing **16** (2): 463–478.

Nielsen, A.A., Conradsen, K. & Simpson, J.J., 1998: Multivariate alteration detection (MAD) and MAF processing in multispectral, bitemporal image data: New approaches to change detection studies. – Remote Sensing of Environment **64:** 1–19.

Niemeyer, I. & Nussbaum, S., 2006: Change detection – the potential for nuclear safeguards. – Verifying Treaty Compliance. Limiting Weapons of Mass Destruction and Monitoring Kyoto Protocol Provisions: 335–348, Springer, Berlin.

Niemeyer, I., Marpu, P.R. & Nussbaum, S., 2008: Change detection using object features. – Object-Based Image Analysis Spatial Concepts for Knowledge-Driven Remote Sensing Applications:185–201, Springer, Berlin.

Niemeyer, I., Bachmann, F., John, A., Listner, C. & Marpu, P.R., 2009: Object-based change detection and classification. – SPIE Europe Remote Sensing 09, Vol. 7477A, Image and Signal Processing for Remote Sensing, Berlin.

Radke, R., Andra, S. & Al-Kofahi, O., 2005: Image change detection algorithms: a systematic survey. – IEEE Transactions on Image Processing **14** (3): 294–307.

Singh, A., 1989: Review Article Digital change detection techniques using remotely-sensed data. – International Journal of Remote Sensing **10** (6): 989–1003.

Walter, V., 2004: Object-based classification of remote sensing data for change detection. – ISPRS Journal of Photogrammetry & Remote Sensing **58:** 225–238.

Zhou, W., Troy, A. & Grove, M., 2008: Object-based Land Cover Classification and Change Analysis in the Baltimore Metropolitan Area Using Multitemporal High Resolution Remote Sensing Data. – Sensors **2008** (8): 1613–1636.

Address of the Authors:

M.Sc. Clemens Listner, Dr. Irmgard Niemeyer, Forschungszentrum Jülich GmbH, Institut für Energie- und Klimaforschung, IEK-6: Nukleare Entsorgung und Reaktorsicherheit, D-52425 Jülich, Tel.: +49-2461-61-8953, -1762, Fax: -2450, e-mail: c.listner@fz-juelich.de, i.niemeyer@fz-juelich.de.

Manuskript eingereicht: März 2011
Angenommen: Mai 2011